Submitted to Physical Review

LBL-280
Preprint

POLARIZATION AND CROSS-SECTION MEASUREMENTS FOR p-^{4}He ELASTIC SCATTERING BETWEEN 20 AND 45 MeV

A. D. Bacher, G. R. Plattner, H. E. Conzett,
D. J. Clark, H. Grunder, and W. F. Tivol

November 1971

AEC Contract No. W-7405-eng-48

DISCLAIMER

POLARIZATION AND CROSS-SECTION MEASUREMENTS FOR p-^{4}He ELASTIC SCATTERING BETWEEN 20 AND 45 MeV*

A. D. Bacher†, G. R. Plattner††, H. E. Conzett,
D. J. Clark, H. Grunder, and W. F. Tivol†††

Lawrence Berkeley Laboratory
University of California
Berkeley, California 94720

November 1971

ABSTRACT

Angular distributions of the polarization and the cross-section for p-^{4}He elastic scattering have been measured in 2 MeV steps between 20 and 45 MeV and in steps of approximately 150 keV across the 23.4 MeV resonance, corresponding to the second excited state of ^{5}Li at 16.7 MeV excitation. The relative uncertainties of the polarization measurements are typically less than ±0.01. The normalization uncertainty from energy to energy and relative to the older data below 20 MeV proton energy is approximately 2%. The cross-section angular distributions with a relative uncertainty of 3% have been normalized to previously existing data, since an absolute cross-section measurement was not feasible with our experimental setup. The polarization measurements provide an accurate proton polarization analyzer up to 45 MeV. With the exception of the narrow resonance region around 23.4 MeV, the analyzing power near $\Theta_{lab} = 125°$ exceeds 80% at all energies and shows no rapid variations. Around 30 MeV, a very weak and broad anomaly is seen in the polarization, coinciding in ^{5}Li excitation (approx. 22 MeV) with the structure observed in d-^{3}He elastic scattering.

I. INTRODUCTION

The low-lying T = 1/2 states of the five nucleon system have been studied extensively and a quantitative understanding of their properties has been achieved.[1] Most recent work has centered around the existence and structure of highly excited T = 1/2 states, particularly in ^{5}Li. A natural way of reaching the excitation energies of interest is to use the d+^{3}He channel which at threshold has an excitation energy of 16.38 MeV. This approach has been widely taken, despite the difficulties which result from the complicated spin structure of the spin 1-spin 1/2 channel. A variety of experimental evidence for excited states in ^{5}Li has been accumulated, but no quantitative explanations have yet been put forth for the anomalies seen in d-^{3}He elastic scattering[2,3] and in the ^{3}He(d,p)^{4}He reaction.[4,5] Progress has been made, but the gap between experiment and theoretical interpretation is still considerable.

The analysis of resonance effects corresponding to states in ^{5}Li will be simplified if they can be observed in the p+^{4}He channel with its single channel spin. States with a structure other than p+^{4}He (i.e. unlike the ground and first excited states of ^{5}Li) will however be only weakly excited via the proton channel. If in addition such states are situated well above the threshold of their main decay channel, they will be very broad and difficult to detect. Indeed, measurements of p-^{4}He cross-section excitation functions[6] do not show any effects corresponding to the structure observed in the d+^{3}He channel.

Since polarization data provide independent information about the scattering amplitudes, a detailed experimental study of p+^{4}He elastic scattering between 20 and 45 MeV was undertaken with particular emphasis on an accurate set of polarization measurements.[7] Cross-section data were also obtained as a

welcome byproduct, but the experimental configuration did not allow comparable precision.

II. EXPERIMENT

A. Apparatus

Both polarization and cross-section measurements were performed simultaneously with the polarized beam from the Berkeley 88-inch cyclotron. The recently installed polarized-ion source of the Saclay-type[10] produced typically 2-3 μA of polarized protons. After the beam was bunched to match the phase acceptance of the cyclotron, it was axially injected and accelerated to the desired energy. The extracted external beam of 80-120 nA was then transported to a 36-inch diameter scattering chamber and focussed onto a target cell containing commercially available high-purity helium. The beam was collimated by a pair of adjustable rectangular slits located approximately 5 m upstream from the target. A second set of 3×6 mm rectangular slits located immediately in front of the target was used to limit the position, direction and size of the beam to values compatible with the overall experimental accuracy. The beam optics were adjusted so that the second slits did not normally intercept the beam.

After passage through the main target, the beam could be slowed down by a set of removeable aluminium absorbers. It then passed through a second helium-filled gas cell used as a polarimeter. A circular collimator was placed just in front of the polarimeter target to produce a well defined beam spot. A split Faraday cup located behind the polarimeter was used to adjust the beam direction before each run. As a result of the additional beam collimation after the primary target, a meaningful beam current integration was not possible.

For this reason, only relative angular distributions of the cross-section could be obtained.

The protons scattered from the primary target were detected in 4 pairs of cooled (-30°C), 5 mm thick, Li-drifted solid-state detectors. The two detectors in each pair were placed at equal angles on opposite sides of the beam. A double slit system was used to limit the angular acceptance of the detectors to approximately ±0.5° in both Θ and azimuthal angle Φ. The angle settings were accurate to better than 0.1°. Above 30 MeV, sets of two stacked 5 mm detectors had to be used at forward angles, where the range of the scattered protons in silicon exceeded 5 mm.

Two monitor detectors, placed left and right of the beam axis at a fixed scattering angle of $\Theta_{lab} = 10°$, served to monitor the incident particle flux for the relative differential cross-section measurements. The proton range was matched to the monitor detector thickness (5 mm) with absorbers.

In the polarimeter a pair of ΔE-E counter telescopes at equal angles on opposite sides of the beam detected the protons scattered from the second helium target. The scattering angle could be varied to correspond to the maximum analyzing efficiency.

B. Polarization Measurements

For each angle setting of the main detector assembly, alternate runs of equal length were taken with the spin vector of the incident beam oriented up and down with respect to the scattering plane. This change of sign of the incident beam polarization was obtained by reversing the magnetic field of the ionizer at the ion source. A test showed that within statistical errors no artificial asymmetry larger than 0.003 was produced by a possible displacement or angular shift of the beam in correlation with the reversal of spin direction.

The polarization $p(\theta)$ was calculated from the ratios of left and right detector yields as described in Ref. 11. The beam polarization was determined from the data taken simultaneously in the polarimeter. While this allowed an accurate monitoring of the beam polarization, a separate experiment was necessary to consistently normalize all of our data to p-^{4}He polarization measurements below 20 MeV (see Sec. III).

All of the polarization data were corrected for the finite geometry of the detection system. The corrections were always less than 0.0025 and thus negligible compared to the statistical errors.

The final relative uncertainties of the polarization data were obtained by quadratically combining the statistical errors of the target and polarimeter yields with the following two contributions: (1) an error corresponding to an uncertainty in scattering angle of $\pm 0.1°$, and (2) an error of ± 0.003 due to a possible correlation between the sign of the incident beam polarization and the position or direction of the beam at the target. We believe that the last two contributions represent a conservative estimate of the systematic errors present.

The absolute normalization of the polarization data will be discussed in Sec. III.

C. Cross-Section Measurements

Cross-section values were obtained from the polarized beam runs by averaging over the spin-up and spin-down runs. As stated before, an absolute determination of the beam intensity was not feasible. In order to extract absolute cross-sections from our relative measurements, it was necessary to normalize to existing data.[6,12]

The final relative errors of the cross-section were obtained by

quadratically combining: (1) the statistical error, (2) the uncertainty in the solid angle of each detector, (3) an error corresponding to an uncertainty in scattering angle of ±0.1°, (4) an uncertainty in the dead-time correction, and (5) an additional contribution for a few forward-angle measurements at the higher energies, where it was evident from the shape of the proton peaks that a small fraction of the particles were not losing their total energy in the sensitive volume of the detectors.

The uncertainty in the absolute normalization was determined from the stated errors of the reference data[6,12] plus an additional contribution due to the possibility of small energy shifts between these measurements and our data.

A particular problem was encountered when we attempted to normalize our cross-section measurements over the sharp resonance structure near 23.4 MeV to those of Ref. 12. It became clear that a systematic energy difference of approximately 150 keV existed between the two sets of data. By shifting the reference data in energy until their energy dependent features coincided with those of our measurements, a tentative normalization could be achieved. It was, however, difficult to derive the associated normalization uncertainty. As a result, the uncertainties we will quote in this region must be taken as an estimate.

In the conversion of all kinematical parameters from the laboratory to the center-of-mass system a relativistic transformation was used.

D. Experimental Procedure

Before and after each run the beam energy was determined by passing the beam through a 110° momentum analyzing magnet.[13] The associated uncertainty of the mean energy is estimated at ±30 keV. The energy spread, deduced from a measurement of the peak-width of protons elastically scattered from a Ni-foil,

is approximately 80 keV (FWHM).

In a first set of runs polarization and cross-section angular distributions were measured in approximately 2 MeV intervals from 20 to 40 MeV. A second set of measurements was performed between 22.5 and 24.5 MeV in steps of approximately 150 keV to determine the effects of the p-^{4}He resonance corresponding to the 16.7 MeV $3/2^+$ level in ^{5}Li. In order to investigate the existence of a weak anomaly discovered near 30 MeV, an excitation function at one angle was then taken from 24 to 30.5 MeV in 0.5 MeV steps. Finally, an absolute normalization of all the measured polarization angular distributions was determined.

III. ABSOLUTE NORMALIZATION OF THE POLARIZATION DATA

It was decided that the polarization in p-^{4}He elastic scattering near 14.5 MeV was sufficiently well known[14,15] and varying slowly enough as a function of energy to constitute an excellent reference on which to base our normalization. A value of $p = -0.771 \pm 0.008$ at $\Theta_{cm} = 80°$ and $E_p = 14.5$ MeV was subsequently used as a reference. This value was deduced from the energy dependent set of phase-shifts of Ref. 15, which in that energy region are based primarily on the data of Ref. 14. The influence of the finite geometry of our polarimeter setup was taken into account. This resulted in a slightly reduced reference value for the polarimeter analyzing power at 14.5 MeV and $\Theta_{cm} = 80°$ of $A = -0.759 \pm 0.011$.

Since it was necessary to reduce the beam energy considerably between the main target and the polarimeter in order to compare our highest energies with 14.5 MeV without too many intermediate steps, a test was performed to check that a large energy degradation would not influence the beam polarization measurements. It is conceivable that changes in beam quality and illumination

of the polarimeter target as well as the greatly increased neutron-induced background in the polarimeter detectors might have affected the measurements. For this test, two runs were made at a proton energy of 45 MeV in the primary target. While monitoring the beam polarization with the main detection system at back angles[16], the polarimeter was run at a fixed angle Θ, first at 37 MeV and then at 30 MeV. Thus, for these two energies the ratio of effective polarimeter analyzing power at the angle Θ could be determined.

A similar set of two runs, both with the beam polarization monitored with the main detection system at 37 MeV, and with the polarimeter run again at the same angle Θ, first at 37 MeV and then at 30 MeV, yielded another independent measurement of the same quantity under very different circumstances (zero absorber thickness at 37 MeV, and roughly half the absorber thickness at 30 MeV). The two numbers thus obtained agreed within the combined statistical uncertainties of 0.4%. From this we concluded that in our setup no undesirable effects would be introduced by the energy degraders.

We then proceeded to the actual normalization of our polarization data relative to the 14.5 MeV reference. A first measurement linked our 20 MeV data to the reference point. The beam polarization was monitored with the main detection system at 20 MeV, while the polarimeter was run first at 20 MeV and then at 14.5 MeV, thus yielding the ratio of the analyzing powers at the angle used ($\Theta_{cm} = 80°$) at these two energies. A second similar measurement was performed with the beam polarization monitored at 30 MeV and the polarimeter run successively at 14.5, 20, 22, 24, 26, 28 and 30 MeV. This yielded another calibration for the 20 MeV data plus one calibration for all the other energies. A third run with the beam polarization monitored at 40 MeV and the polarimeter

run at 26, 28, 30, 32, 34, 37 and 40 MeV finally linked the remaining energies to our reference point, yielding in addition a second independent calibration for the 26, 28 and 30 MeV data.

The 10 polarization angular distributions across the 23.4 MeV resonance were not normalized in this manner, since it would have been impossible to slow the protons to exactly the proper energy, quite apart from the danger of introducing too large an energy spread compared to the resonance width. When these data were taken between 22.5 and 24.5 MeV, the polarimeter ran (with a fixed absorber thickness) about 2.5 MeV lower (i.e. between 20 and 22 MeV). The measurements already normalized at 20 and 22 MeV were therefore used to obtain the proper polarimeter analyzing power by interpolation.

The actual energies used were, of course, the precise energies at which the angular distributions had previously been measured (see Tables I and II). The proton ranges from which we calculated the necessary absorber thicknesses were taken from Ref. 17.

The uncertainties in normalization as listed in Tables I and II are the quadratic combination of the statistical errors of the normalization measurements and the uncertainty of the reference point.

IV. RESULTS

The numerical results of all our measurements are presented in Tables I-VI.

Figs. 1 and 2 show four typical angular distributions of the polarization $p(\theta)$ and the differential cross-section $\sigma(\theta)$. In Fig. 3, excitation functions of the polarization across the narrow resonance near 23 MeV are shown for 3 of the 15 angles investigated. The dashed lines are intended as a

guide to the eye. Fig. 4 presents the excitation function of the polarization taken at $\Theta_{cm} = 102.2°$ across the weak anomaly near 28-30 MeV. The sharp structure near 23.4 MeV is due to the $3/2^+$ level at 16.7 MeV excitation in ^{5}Li, and the broad bump around 30 MeV corresponds in ^{5}Li excitation to the structure observed in the d-^{3}He elastic scattering cross-section.[2] For comparison, a d-^{3}He cross-section excitation function at $\Theta_{cm} = 90°$ is plotted in the insert.

A contour plot of the experimental polarization between 16 and 45 MeV is shown in Fig. 5. The data below 20 MeV are taken from Refs. 14 and 15.

The match between our polarization data and the existing data below 20 MeV is excellent. The same comment also applies at the higher energies, though we do not show any comparisons. Both double-scattering measurements[18,19] as well as older data obtained with a polarized-ion source[20,22] generally agree with our data within statistical errors. It is particularly gratifying to note the excellent agreement in absolute normalization between our data and the RHEL data[21,22] near 29 and 40 MeV, since the two sets were normalized according to quite different standards.

Our cross-section measurements have been compared to older, less abundant, but in general more accurate data[12,20,22-24] wherever possible. The angular distributions are in reasonable agreement, but in some instances there exist differences in the absolute normalization of up to 10%. The quoted systematic normalization errors of the different sets of data can in general explain these discrepancies, though from the point of view of a future analysis this is of course an unfortunate situation.

V. DISCUSSION

The measured polarization as presented in this report behaves very smoothly as a function of energy at all angles, including those which provide

the best figure of merit for a polarization analyzer (i.e. the negative and positive maxima near $\Theta_{lab} = 80°$ and 125°, respectively).

We believe that the amount and precision of our polarization data permit the calibration of an efficient polarization analyzer to better than 3% by simple interpolation in energy and angle (except of course in a 2 MeV wide region around the resonance near 23.4 MeV). In view of the internal consistency of our data, we find it doubtful that an energy dependent analysis of the type now fashionable[15,25] could lead to uncertainties significantly lower than those of our data (upon which it would presumably have to be based). Of course, we do not intend to belittle the value of such an analysis, especially where it might provide new insights into the physics of the process investigated.

As shown in Figs. 4 and 5, a very weak and broad anomaly in the p-^{4}He polarization exists near 30 MeV. This energy corresponds to an excitation in ^{5}Li of approximately 22 MeV. As we have already mentioned, the anomaly is so weak that it is not observed in the p-^{4}He cross-section.[6] This is in contrast to d-^{3}He elastic scattering where a strong "resonance-like" behaviour has been found both with unpolarized[2] and polarized[3] deuterons. From these facts it must be concluded, that the structure of ^{5}Li between 18 and 32 MeV excitation energy is not of p+^{4}He character as it is for the ground and first excited states. Some coupling to the p+^{4}He channel does exist, but the structure of ^{5}Li in this energy region is more likely of the d+^{3}He type. These experimental conclusions (which are by no means new) agree very well with recent theoretical calculations of ^{5}Li structure above the d+^{3}He threshold.[26]

While there can be little doubt that a phase-shift analysis of our data will lead to a better understanding of the p-^{4}He elastic scattering process in this energy region, it remains to be seen to what extent quantitative

information about the structure of ^{5}Li can be obtained. Such a discussion of our experimental results will be the subject of a separate paper.[27]

VI. ACKNOWLEDGMENTS

We wish to express our thanks to the staff of the 88-inch cyclotron for their efficient operation of the accelerator. In addition, we are indebted to Prof. W. Haeberli for valuable discussions, and to Profs. P. Schwandt and J. W. Verba for sending us results of their work prior to publication.

FOOTNOTES AND REFERENCES

* Work performed under the auspices of the U. S. Atomic Energy Commission.

† Present address: Physics Department, Indiana University, Bloomington, Indiana 47401.

†† Present address: Physics Department, University of Basel, 4056 Basel, Switzerland.

††† Present address: Sealy Mudd Laboratory, Los Angeles, California 90033.

1. T. Lauritsen and F. Ajzenberg-Selove, Nucl. Phys. 78, 1 (1966).

2. T. A. Tombrello, R. J. Spiger, and A. D. Bacher, Phys. Rev. 154, 935 (1967).

3. V. König, W. Grüebler, R. E. White, P. A. Schmelzbach, and P. Marmier, Proceedings of the Third International Symposium on Polarization Phenomena in Nuclear Reactions, Madison 1970, edited by H. H. Barschall and W. Haeberli (University of Wisconsin Press, Madison, 1970) p. 526.

4. L. Stewart, J. E. Brolley, and L. Rosen, Phys. Rev. 119, 1649 (1960).

5. W. Grüebler, V. König, A. Ruh, P. A. Schmelzbach, and R. E. White, Proc. Third Pol. Symp., ref. cit., p. 543.

6. S. N. Bunker, J. M. Cameron, M. B. Epstein, G. Paic, J. Reginald Richardson, J. G. Rogers, P. Tomas, and J. W. Verba, Nucl. Phys. A133, 537 (1969).

7. According to the Madison Convention[8], the quantity which we have measured should be called the analyzing power. Since for $p+^4He$ elastic scattering parity conservation requires equality in sign and magnitude between the analyzing power and the proton polarization, we shall use the more conventional term polarization. In every other respect we follow the Basel[9] and Madison Conventions.

8. Proc. Third Pol. Symp., ref. cit., p.XXV.

9. Proceedings of the International Conference on Polarization Phenomena of Nucleons, Basel, Switzerland, 1960, edited by P. Huber and K. P. Meyer (Helv. Phys. Acta Suppl. VI, 1961) p. 436.

10. D. J. Clark, A. U. Lucchio, F. Resmini, and H. Meiner, Proceedings of the Fifth International Cyclotron Conference, 1969 (Butterworth, London, England, 1971) p. 610.

11. G. R. Plattner, T. B. Clegg, and L. G. Keller, Nucl. Phys. A111, 481 (1968).

12. P. W. Allison and R. Smythe, Nucl. Phys. A121, 97 (1968).

13. R. E. Hintz, F. B. Selph, W. S. Flood, B. G. Harvey, F. G. Resmini, and E. A. McClatchie, Nucl. Instr. Meth. 72, 61 (1969).

14. D. Garreta, J. Sura, and A. Tarrats, Nucl. Phys. A132, 204 (1969).

15. P. Schwandt, T. B. Clegg, and W. Haeberli, Nucl. Phys. A163, 432 (1971).

16. These measurements were subsequently used to extend the range of accurately known polarization over the backward peak up to 45 MeV, as shown in Fig. 5.

17. J. F. Janni, Technical report No. AFWL-TR-65-150, obtained from Clearinghouse, U. S. Dept. of Commerce, Washington, U. S. A.

18. W. G. Weitkamp and W. Haeberli, Nucl. Phys. 83, 46 (1966).

19. E. T. Boschitz, M. Chabre, H. E. Conzett, E. Shield, and R. J. Slobodrian, Proceedings of the Second International Symposium on Polarization Phenomena of Nucleons, Karlsruhe, Germany, 1965, edited by P. Huber and H. Schopper (Experienta Suppl. 12, 1966) p. 328; and Phys. Lett. 15, 325 (1965).

20. P. Darriulat, D. Garreta, A. Tarrats, and J. Testoni, Nucl. Phys. A108, 316 (1968).

21. M. K. Craddock, R. C. Hanna, L. P. Robertson, and B. W. Davies, Phys. Lett. 5, 335 (1963).

22. D. J. Plummer, K. Ramavataram, T. A. Hodges, D. G. Montague, A. Zucker, and N. K. Ganguly, Nucl. Phys. A174, 193 (1971).

23. S. M. Bunch, H. H. Forster, and C. C. Kim, Nucl. Phys. 53, 241 (1964).

24. M. K. Brussel and J. H. Williams, Phys. Rev. 106, 286 (1957).

25. R. A. Arndt, L. D. Roper, and R. L. Shotwell, Phys. Rev. C3, 2100 (1971).

26. P. Heiss and H. Hackenbroich, Nucl. Phys. A162, 530 (1971).

27. G. R. Plattner, A. D. Bacher, and H. E. Conzett, to be submitted to Physical Review.

TABLE I. Proton polarization in p-^{4}He elastic scattering from 19.94 to 39.80 MeV proton lab. energy.

θ_{lab}	θ_{cm}	19.94	21.90	23.98	25.82	28.13
17.5°	21.9°	−0.083 ± 0.006	−0.091 ± 0.004	−0.041 ± 0.004	−0.038 ± 0.005	0.001 ± 0.004
27.5°	34.2°	−0.168 ± 0.005	−0.166 ± 0.005[a]	−0.085 ± 0.004[a]	−0.073 ± 0.005[a]	−0.026 ± 0.004[a]
37.5°	46.4°	−0.245 ± 0.006	−0.236 ± 0.005	−0.144 ± 0.005	−0.128 ± 0.005	−0.082 ± 0.005
47.5°	58.3°	−0.333 ± 0.008	−0.332 ± 0.006	−0.230 ± 0.006	−0.196 ± 0.007	−0.142 ± 0.005[a]
57.5°	69.9°	−0.438 ± 0.005	−0.437 ± 0.005	−0.357 ± 0.005	−0.302 ± 0.005	−0.241 ± 0.005
67.5°	81.1°	−0.560 ± 0.006	−0.540 ± 0.005	−0.514 ± 0.005	−0.458 ± 0.006	−0.365 ± 0.005
77.5°	91.9°	−0.671 ± 0.007	−0.621 ± 0.007	−0.624 ± 0.007	−0.572 ± 0.008	−0.477 ± 0.007
82.3°	96.9°	−0.669 ± 0.006	−0.606 ± 0.005	−0.567 ± 0.006	−0.553 ± 0.006	−0.462 ± 0.006
87.5°	102.2°	−0.539 ± 0.009	−0.479 ± 0.009	−0.363 ± 0.010	−0.369 ± 0.011	−0.270 ± 0.010
92.3°	107.0°	−0.264 ± 0.010	−0.195 ± 0.010	−0.065 ± 0.009	−0.084 ± 0.009	0.012 ± 0.009
97.5°	112.1°	0.227 ± 0.012	0.310 ± 0.013	0.299 ± 0.011	0.302 ± 0.012	0.372 ± 0.010
102.3°	116.7°	0.682 ± 0.010	0.706 ± 0.009	0.566 ± 0.007	0.591 ± 0.009	0.616 ± 0.008
107.5°	121.5°	0.913 ± 0.009	0.911 ± 0.009	0.758 ± 0.008	0.785 ± 0.010	0.768 ± 0.008[a]
112.3°	125.9°	0.931 ± 0.007	0.899 ± 0.008	0.800 ± 0.007	0.847 ± 0.008	0.815 ± 0.007
117.5°	130.5°	0.863 ± 0.008	0.824 ± 0.008	0.812 ± 0.008	0.863 ± 0.009	0.831 ± 0.008
120.0°	132.7°	0.817 ± 0.008	0.766 ± 0.008	0.799 ± 0.008	0.829 ± 0.008	0.817 ± 0.008
127.5°	139.1°	0.657 ± 0.007	0.605 ± 0.007	0.716 ± 0.007	0.738 ± 0.008	0.765 ± 0.008
130.0°	141.2°	0.612 ± 0.007	0.557 ± 0.007	0.690 ± 0.008	0.711 ± 0.008	0.747 ± 0.007
140.0°	149.4°	0.443 ± 0.006	0.391 ± 0.006	0.560 ± 0.007	0.541 ± 0.008	0.640 ± 0.007
150.0°	157.3°	0.312 ± 0.005	0.266 ± 0.006	0.414 ± 0.006	0.409 ± 0.007	0.529 ± 0.006
Normalization uncertainty		± 1.5 %	± 2.2 %	± 2.1 %	± 2.3 %	± 2.5 %

TABLE I. (cont'd)

θ_{lab}	$\theta_{c.m.}$	30.43	32.17	34.30	36.93	39.80
17.5°	21.9°	0.014 ± 0.004	0.023 ± 0.005	0.020 ± 0.004	0.034 ± 0.005	0.039 ± 0.006
27.5°	34.3°	−0.015 ± 0.004	−0.007 ± 0.005	0.002 ± 0.004	0.019 ± 0.004	0.025 ± 0.005
37.5°	46.5°	−0.059 ± 0.005	−0.037 ± 0.005	−0.039 ± 0.005	−0.027 ± 0.005	−0.027 ± 0.007
47.5°	58.4°	−0.125 ± 0.006	−0.107 ± 0.007	−0.091 ± 0.007	−0.070 ± 0.007	−0.062 ± 0.007
57.5°	69.9°	−0.211 ± 0.005	−0.198 ± 0.005	−0.163 ± 0.005[a]	−0.128 ± 0.005[a]	−0.091 ± 0.005[a]
67.5°	81.1°	−0.341 ± 0.005	−0.322 ± 0.006	−0.263 ± 0.006[a]	−0.200 ± 0.006[a]	−0.145 ± 0.007[a]
77.5°	91.9°	−0.450 ± 0.007	−0.441 ± 0.008	−0.370 ± 0.008	−0.333 ± 0.008[a]	−0.239 ± 0.008[a]
82.3°	96.9°	−0.433 ± 0.006	−0.438 ± 0.008	−0.411 ± 0.007[a]	−0.372 ± 0.009[a]	−0.332 ± 0.007[a]
87.5°	102.2°	−0.278 ± 0.010	−0.323 ± 0.012[a]	−0.355 ± 0.010[a]	−0.391 ± 0.010[a]	−0.383 ± 0.012[a]
92.3°	107.0°	−0.020 ± 0.010	−0.127 ± 0.011[a]	−0.208 ± 0.009[a]	−0.326 ± 0.010[a]	−0.376 ± 0.011[a]
97.5°	112.1°	0.297 ± 0.011	0.193 ± 0.014	0.027 ± 0.013[a]	−0.162 ± 0.013[a]	−0.260 ± 0.015[a]
102.3°	116.7°	0.527 ± 0.009	0.408 ± 0.010	0.252 ± 0.010	0.072 ± 0.012[a]	−0.074 ± 0.011[a]
107.5°	121.6°	0.678 ± 0.008	0.581 ± 0.012	0.453 ± 0.012	0.289 ± 0.012	0.137 ± 0.012
112.3°	125.9°	0.774 ± 0.008	0.722 ± 0.008	0.610 ± 0.009	0.503 ± 0.012[a]	0.406 ± 0.012[a]
117.5°	130.5°	0.795 ± 0.008	0.817 ± 0.010[a]	0.753 ± 0.010[a]	0.650 ± 0.012[a]	0.627 ± 0.012[a]
120.0°	132.7°	0.827 ± 0.008	0.821 ± 0.009	0.770 ± 0.010[a]	0.739 ± 0.011[a]	0.710 ± 0.012[a]
127.5°	139.1°	0.831 ± 0.008	0.856 ± 0.010[a]	0.841 ± 0.010[a]	0.858 ± 0.010[a]	0.870 ± 0.012[a]
130.0°	141.2°	0.808 ± 0.008	0.835 ± 0.008	0.837 ± 0.009[a]	0.867 ± 0.010[a]	0.885 ± 0.010[a]
140.0°	149.4°	0.742 ± 0.008	0.790 ± 0.008	0.789 ± 0.009	0.818 ± 0.009	0.840 ± 0.009
150.0°	157.3°	0.621 ± 0.008	0.655 ± 0.011	0.630 ± 0.009	0.637 ± 0.008	0.651 ± 0.008
Normalization uncertainty		±1.6 %	±2.9 %	±2.4 %	±2.4 %	±1.8 %

[a] Increase $\theta_{c.m.}$ by 0.1° from value listed in second column.

TABLE II. Proton polarization in p-^{4}He elastic scattering from 22.46 to 24.51 MeV proton lab. energy.

θ_{lab}	θ_{cm}	22.46	22.71	22.96	23.16	23.29
17.5°	21.9°	-0.087 ± 0.004	-0.109 ± 0.004	-0.120 ± 0.004	-0.138 ± 0.004	-0.115 ± 0.005
27.5°	34.3°	-0.185 ± 0.004	-0.193 ± 0.004	-0.213 ± 0.005	-0.228 ± 0.004	-0.194 ± 0.008
37.5°	46.4°	-0.257 ± 0.005	-0.270 ± 0.005	-0.303 ± 0.006	-0.333 ± 0.006	-0.276 ± 0.005
47.5°	58.3°	-0.351 ± 0.007	-0.368 ± 0.006	-0.387 ± 0.008	-0.433 ± 0.007	-0.392 ± 0.007
57.5°	69.9°	-0.441 ± 0.005	-0.442 ± 0.006	-0.465 ± 0.006	-0.516 ± 0.006	-0.520 ± 0.006
67.5°	81.1°	-0.528 ± 0.007	-0.524 ± 0.007	-0.528 ± 0.007	-0.547 ± 0.007	-0.579 ± 0.007
77.5°	91.9°	-0.580 ± 0.008	-0.546 ± 0.008	-0.507 ± 0.009	-0.431 ± 0.008	-0.427 ± 0.009
87.5°	102.2°	-0.415 ± 0.009	-0.350 ± 0.009	-0.273 ± 0.009	-0.037 ± 0.012	0.094 ± 0.008
97.5°	112.1°	0.325 ± 0.014	0.417 ± 0.013	0.479 ± 0.013	0.676 ± 0.015	0.587 ± 0.009
107.5°	121.5°	0.913 ± 0.013	0.877 ± 0.012	0.841 ± 0.011	0.747 ± 0.010	0.631 ± 0.009
117.5°	130.5°	0.776 ± 0.010	0.702 ± 0.010	0.633 ± 0.011	0.439 ± 0.009	0.465 ± 0.008
120.0°	132.7°	0.702 ± 0.012	0.681 ± 0.012	0.551 ± 0.012	0.377 ± 0.011	0.429 ± 0.010
130.0°	141.2°	0.494 ± 0.010	0.441 ± 0.009	0.362 ± 0.010	0.182 ± 0.009	0.296 ± 0.009
140.0°	149.4°	0.340 ± 0.008	0.297 ± 0.008	0.211 ± 0.009	0.073 ± 0.008	0.192 ± 0.008
150.0°	157.3°	0.231 ± 0.007	0.184 ± 0.007	0.135 ± 0.007	0.020 ± 0.006	0.108 ± 0.007
Normalization uncertainty		± 1.6 %	± 1.6 %	± 1.7 %	± 1.8 %	± 1.9 %

θ_{lab}	θ_{cm}	23.48	23.56	23.70	23.85	24.51
17.5°	21.9°	-0.042 ± 0.004	-0.038 ± 0.004	-0.032 ± 0.004	-0.039 ± 0.004	-0.044 ± 0.004
27.5°	34.3°	-0.078 ± 0.006	-0.081 ± 0.004	-0.080 ± 0.004	-0.085 ± 0.004	-0.086 ± 0.005
37.5°	46.4°	-0.144 ± 0.005	-0.143 ± 0.005	-0.136 ± 0.005	-0.142 ± 0.004	-0.148 ± 0.004
47.5°	58.3°	-0.239 ± 0.006	-0.243 ± 0.007	-0.240 ± 0.007	-0.241 ± 0.006	-0.234 ± 0.006
57.5°	69.9°	-0.398 ± 0.005	-0.380 ± 0.005	-0.371 ± 0.005	-0.358 ± 0.005	-0.354 ± 0.005
67.5°	81.1°	-0.562 ± 0.007	-0.547 ± 0.007	-0.528 ± 0.007	-0.517 ± 0.006	-0.507 ± 0.007
77.5°	91.9°	-0.618 ± 0.008	-0.614 ± 0.008	-0.616 ± 0.008	-0.630 ± 0.008	-0.626 ± 0.008
87.5°	102.2°	-0.253 ± 0.008	-0.281 ± 0.009	-0.322 ± 0.011	-0.370 ± 0.008	-0.393 ± 0.011
97.5°	112.1°	0.388 ± 0.010	0.368 ± 0.010	0.352 ± 0.010	0.319 ± 0.010	0.289 ± 0.014
107.5°	121.5°	0.715 ± 0.010	0.718 ± 0.009	0.731 ± 0.011	0.753 ± 0.009	0.751 ± 0.012
117.5°	130.5°	0.760 ± 0.009	0.763 ± 0.008	0.787 ± 0.008	0.820 ± 0.008	0.817 ± 0.013
120.0°	132.7°	0.745 ± 0.010	0.756 ± 0.009	0.772 ± 0.009	0.803 ± 0.009	0.815 ± 0.010
130.0°	141.2°	0.659 ± 0.009	0.670 ± 0.008	0.689 ± 0.008	0.687 ± 0.009	0.707 ± 0.009
140.0°	149.4°	0.561 ± 0.011	0.553 ± 0.008	0.563 ± 0.008	0.560 ± 0.008	0.568 ± 0.009
150.0°	157.3°	0.427 ± 0.008	0.434 ± 0.007	0.429 ± 0.007	0.416 ± 0.007	0.396 ± 0.007
Normalization uncertainty		± 1.9 %	± 2.0 %	± 2.1 %	± 2.1 %	± 2.2 %

TABLE III. Cross-section (mb/sr) in p-^{4}He elastic scattering from 19.94 to 39.80 MeV proton lab. energy.

θ_{lab}	θ_{cm}	19.94	21.90	23.98	25.82	28.13
17.5°	21.9°	180.20 ± 2.5 %	167.50 ± 2.5 %	176.00 ± 4.5 %	162.00 ± 4.5 %	162.10 ± 3.5 %
27.5°	34.2°	163.60 ± 3.0 %	153.50 ± 3.0 %[a]	150.00 ± 4.0 %[a]	133.80 ± 4.5 %[a]	135.80 ± 3.5 %[a]
37.5°	46.4°	128.80 ± 2.5 %	120.40 ± 2.5 %	110.80 ± 2.5 %	96.10 ± 3.0 %	86.10 ± 3.0 %
47.5°	58.3°	91.90 ± 3.5 %	84.30 ± 3.5 %	72.10 ± 3.5 %	62.00 ± 3.5 %	52.50 ± 4.0 %[a]
57.5°	69.9°	57.10 ± 2.5 %	51.40 ± 2.5 %	42.40 ± 2.5 %	36.60 ± 2.5 %	29.60 ± 2.5 %
67.5°	81.1°	34.70 ± 3.0 %	32.00 ± 3.0 %	24.30 ± 3.0 %	21.50 ± 3.0 %	16.90 ± 3.5 %
77.5°	91.9°	18.20 ± 3.0 %	17.00 ± 3.0 %	12.90 ± 3.0 %	11.40 ± 3.0 %	8.83 ± 4.0 %
82.3°	96.9°	13.10 ± 2.5 %	11.80 ± 2.5 %	9.52 ± 2.5 %	8.53 ± 2.5 %	6.29 ± 3.0 %
87.5°	102.2°	9.09 ± 3.5 %	8.22 ± 3.5 %	7.68 ± 3.5 %	6.73 ± 3.5 %	5.23 ± 4.5 %
92.3°	107.0°	6.89 ± 3.0 %	6.34 ± 3.0 %	6.73 ± 3.0 %	5.96 ± 3.0 %	4.60 ± 3.5 %
97.5°	112.1°	5.66 ± 2.5 %	5.07 ± 2.5 %	6.36 ± 2.5 %	5.54 ± 2.5 %	4.63 ± 3.0 %
102.3°	116.7°	5.97 ± 3.0 %	5.28 ± 3.0 %	7.06 ± 2.5 %	6.16 ± 2.5 %	5.26 ± 3.0 %
107.5°	121.5°	7.10 ± 3.0 %	6.13 ± 3.0 %	8.11 ± 3.0 %	6.93 ± 3.5 %	6.07 ± 3.5 %[a]
112.3°	125.9°	9.12 ± 3.5 %	8.07 ± 3.5 %	9.49 ± 3.5 %	8.20 ± 3.5 %	7.11 ± 3.5 %
117.5°	130.5°	11.50 ± 2.5 %	10.20 ± 2.5 %	10.90 ± 2.5 %	9.39 ± 2.5 %	8.23 ± 3.0 %
120.0°	132.7°	12.50 ± 2.5 %	11.00 ± 2.5 %	11.30 ± 2.5 %	9.92 ± 2.5 %	8.48 ± 2.5 %
127.5°	139.1°	17.90 ± 3.5 %	15.80 ± 3.5 %	14.20 ± 3.5 %	12.30 ± 3.5 %	10.30 ± 3.5 %
130.0°	141.2°	19.30 ± 3.0 %	17.00 ± 3.0 %	14.90 ± 3.0 %	13.00 ± 3.0 %	10.50 ± 3.0 %
140.0°	149.4°	26.20 ± 2.5 %	23.00 ± 2.5 %	17.80 ± 2.5 %	15.60 ± 2.5 %	11.50 ± 3.0 %
150.0°	157.3°	32.40 ± 3.5 %	28.20 ± 3.5 %	20.50 ± 3.5 %	17.70 ± 3.5 %	12.60 ± 3.5 %
Normalization uncertainty		± 5.0 %	± 5.0 %	± 4.0 %	± 4.0 %	± 3.0 %

TABLE III. (cont'd)

θ_{lab}	θ_{cm}	30.43	32.17	34.30	36.93	39.80
17.5°	21.9°	173.70 ± 3.0 %	177.30 ± 4.0 %	187.20 ± 4.5 %		
27.5°	34.3°	137.60 ± 3.0 %	127.20 ± 3.5 %	129.70 ± 4.5 %	114.50 ± 3.5 %	107.50 ± 4.0 %
37.5°	46.5°	83.10 ± 3.0 %	75.20 ± 3.0 %	71.10 ± 3.0 %	58.10 ± 3.5 %	51.40 ± 3.5 %
47.5°	58.4°	47.60 ± 3.5 %	40.10 ± 4.0 %	34.90 ± 3.5 %	27.60 ± 4.0 %	22.50 ± 4.0 %
57.5°	69.9°	24.00 ± 2.5 %	20.30 ± 4.0 %	16.50 ± 4.0 %[a]	12.70 ± 4.5 %[a]	9.32 ± 5.0 %[a]
67.5°	81.1°	13.50 ± 3.0 %	10.90 ± 3.5 %	8.80 ± 3.5 %[a]	6.58 ± 3.5 %[a]	4.94 ± 4.0 %[a]
77.5°	91.9°	7.07 ± 3.0 %	5.85 ± 3.0 %	4.74 ± 3.0 %	3.69 ± 3.0 %[a]	2.92 ± 3.0 %[a]
82.3°	96.9°	5.00 ± 2.5 %	4.28 ± 3.0 %	3.59 ± 3.0 %[a]	2.92 ± 3.0 %[a]	2.34 ± 3.0 %[a]
87.5°	102.2°	4.16 ± 3.5 %	3.57 ± 3.5 %[a]	3.06 ± 3.5 %[a]	2.55 ± 3.5 %[a]	2.12 ± 4.0 %[a]
92.3°	107.0°	3.80 ± 3.0 %	3.19 ± 3.5 %[a]	2.74 ± 3.5 %[a]	2.34 ± 3.5 %[a]	1.89 ± 3.5 %[a]
97.5°	112.1°	3.77 ± 2.5 %	3.26 ± 2.5 %	2.74 ± 2.5 %[a]	2.19 ± 2.5 %[a]	1.83 ± 3.0 %[a]
102.3°	116.7°	4.34 ± 3.0 %	3.70 ± 3.0 %	3.05 ± 3.0 %	2.51 ± 3.0 %[a]	1.95 ± 3.0 %[a]
107.5°	121.6°	4.97 ± 3.0 %	4.14 ± 3.5 %	3.37 ± 3.0 %	2.65 ± 3.5 %	2.04 ± 3.5 %
112.3°	125.9°	5.52 ± 3.5 %	5.06 ± 3.5 %	4.03 ± 3.5 %	3.15 ± 3.5 %[a]	2.34 ± 3.5 %[a]
117.5°	130.5°	6.53 ± 3.0 %	5.56 ± 3.0 %[a]	4.49 ± 3.0 %[a]	3.44 ± 3.0 %[a]	2.55 ± 3.0 %[a]
120.0°	132.7°	6.70 ± 2.5 %	5.88 ± 2.5 %	4.60 ± 2.5 %[a]	3.51 ± 2.5 %[a]	2.65 ± 3.0 %[a]
127.5°	139.1°	8.17 ± 3.5 %	6.98 ± 3.5 %[a]	5.73 ± 3.5 %[a]	4.54 ± 3.5 %[a]	3.41 ± 3.5 %[a]
130.0°	141.2°	8.51 ± 3.0 %	7.26 ± 3.0 %	5.91 ± 3.0 %[a]	4.76 ± 3.0 %[a]	3.76 ± 3.0 %[a]
140.0°	149.4°	9.49 ± 3.0 %	8.64 ± 3.0 %	7.36 ± 2.5 %	6.36 ± 2.5 %	5.39 ± 3.0 %
150.0°	157.3°	10.30 ± 3.5 %	9.73 ± 3.5 %	8.88 ± 3.5 %	8.27 ± 3.5 %	7.24 ± 3.5 %
Normalization uncertainty		±3.5 %	±4.0 %	±3.0 %	±3.0 %	±4.0 %

[a] Increase θ_{cm} by 0.1° from value listed in second column.

TABLE IV. Cross-section (mb/sr) in p-^{4}He elastic scattering from 22.46 to 24.51 MeV proton lab. energy.

θ_{lab}	θ_{cm}	22.46	22.71	22.96	23.16	23.29
17.5°	21.9°	175.00 ± 3.5 %	175.00 ± 3.5 %	175.00 ± 3.0 %	193.00 ± 3.0 %	200.00 ± 3.0 %
27.5°	34.3°	145.00 ± 3.0 %	139.00 ± 2.5 %	139.00 ± 3.0 %	149.00 ± 3.0 %	157.00 ± 3.0 %
37.5°	46.4°	112.00 ± 3.0 %	106.00 ± 2.5 %	105.00 ± 3.0 %	111.00 ± 3.0 %	114.00 ± 3.0 %
47.5°	58.3°	77.30 ± 2.5 %	74.00 ± 2.5 %	71.90 ± 2.5 %	74.30 ± 2.5 %	71.10 ± 2.5 %
57.5°	69.9°	50.00 ± 2.5 %	49.70 ± 2.5 %	47.50 ± 3.0 %	47.20 ± 2.5 %	42.30 ± 3.0 %
67.5°	81.1°	28.70 ± 2.5 %	28.50 ± 2.5 %	27.00 ± 2.5 %	26.40 ± 2.5 %	21.90 ± 3.0 %
77.5°	91.9°	15.10 ± 2.5 %	15.20 ± 3.0 %	14.50 ± 3.0 %	13.90 ± 3.0 %	11.60 ± 3.0 %
87.5°	102.2°	7.41 ± 3.0 %	7.37 ± 3.0 %	6.85 ± 3.0 %	6.95 ± 3.0 %	6.98 ± 3.0 %
97.5°	112.1°	4.51 ± 3.0 %	4.44 ± 3.0 %	4.09 ± 2.5 %	4.34 ± 3.0 %	6.27 ± 2.5 %
107.5°	121.5°	5.44 ± 3.0 %	5.36 ± 3.0 %	4.84 ± 3.0 %	5.35 ± 3.0 %	7.74 ± 2.5 %
117.5°	130.5°	8.79 ± 2.5 %	8.74 ± 2.5 %	7.96 ± 2.5 %	8.19 ± 2.5 %	10.00 ± 2.5 %
120.0°	132.7°	10.00 ± 2.5 %	9.60 ± 3.0 %	8.90 ± 3.0 %	8.97 ± 3.0 %	11.00 ± 3.0 %
130.0°	141.2°	14.30 ± 2.5 %	14.10 ± 2.5 %	12.90 ± 2.5 %	12.80 ± 2.5 %	13.10 ± 2.5 %
140.0°	149.4°	19.40 ± 2.5 %	19.00 ± 2.5 %	17.50 ± 2.5 %	16.60 ± 3.0 %	14.80 ± 2.5 %
150.0°	157.3°	24.40 ± 2.5 %	24.30 ± 2.5 %	21.70 ± 2.5 %	20.50 ± 2.5 %	16.10 ± 2.5 %
Normalization uncertainty		± 5.0 %	± 5.0 %	± 5.0 %	± 5.0 %	± 5.0 %

θ_{lab}	θ_{cm}	23.48	23.56	23.70	23.85	24.51
17.5°	21.9°	193.00 ± 3.0 %	193.00 ± 3.0 %	180.00 ± 3.0 %	185.00 ± 3.0 %	173.00 ± 3.0 %
27.5°	34.3°	148.00 ± 3.0 %	152.00 ± 3.0 %	141.00 ± 3.0 %	142.00 ± 3.0 %	135.00 ± 3.0 %
37.5°	46.4°	107.00 ± 3.0 %	111.00 ± 3.0 %	104.00 ± 3.0 %	106.00 ± 3.0 %	99.30 ± 3.0 %
47.5°	58.3°	68.50 ± 3.0 %	71.80 ± 3.0 %	67.50 ± 3.0 %	68.70 ± 2.0 %	64.70 ± 3.0 %
57.5°	69.9°	43.20 ± 3.0 %	41.40 ± 3.0 %	41.90 ± 3.0 %	41.60 ± 3.0 %	39.80 ± 3.0 %
67.5°	81.1°	22.40 ± 2.5 %	22.20 ± 3.0 %	22.10 ± 3.0 %	22.20 ± 2.5 %	21.70 ± 3.0 %
77.5°	91.9°	12.00 ± 3.0 %	11.80 ± 3.0 %	11.90 ± 3.0 %	11.90 ± 3.0 %	11.70 ± 3.0 %
87.5°	102.2°	7.55 ± 3.0 %	7.36 ± 3.0 %	7.26 ± 3.0 %	7.16 ± 3.0 %	6.82 ± 3.0 %
97.5°	112.1°	7.11 ± 2.5 %	6.73 ± 2.5 %	6.50 ± 2.5 %	6.09 ± 2.5 %	5.57 ± 3.0 %
107.5°	121.5°	8.81 ± 2.5 %	8.59 ± 2.5 %	7.82 ± 3.0 %	7.57 ± 2.5 %	6.96 ± 3.0 %
117.5°	130.5°	11.50 ± 2.5 %	11.00 ± 2.5 %	10.70 ± 2.5 %	10.30 ± 2.5 %	9.34 ± 3.0 %
120.0°	132.7°	11.80 ± 3.0 %	11.30 ± 3.0 %	11.40 ± 3.0 %	11.20 ± 2.5 %	10.30 ± 3.0 %
130.0°	141.2°	14.10 ± 2.5 %	13.60 ± 2.5 %	13.80 ± 2.5 %	14.20 ± 2.5 %	12.90 ± 3.0 %
140.0°	149.4°	16.00 ± 3.0 %	15.80 ± 2.5 %	16.30 ± 2.5 %	16.90 ± 2.5 %	15.80 ± 3.0 %
150.0°	157.3°	18.20 ± 2.5 %	17.60 ± 2.5 %	18.50 ± 2.5 %	19.50 ± 2.5 %	18.60 ± 2.5 %
Normalization uncertainty		± 5.0 %	± 5.0 %	± 5.0 %	± 5.0 %	± 5.0 %

TABLE V. Proton polarization in p-^{4}He elastic scattering at 45.04 MeV proton lab. energy.

θ_{lab}	θ_{cm}	$p(\theta)$
120.0°	132.8°	0.610 ± 0.012
130.0°	141.3°	0.926 ± 0.010
140.0°	149.4°	0.847 ± 0.008
150.0°	157.3°	0.644 ± 0.007
Normalization uncertainty		± 1.5 %

TABLE VI. Proton polarization in p-^{4}He elastic scattering at θ_{cm} = 102.2° from 24.0 to 30.2 MeV proton lab. energy.

E_p (MeV)	$p(102.2^\circ)$
24.0	-0.349 ± 0.009
24.5	-0.389 ± 0.009
25.0	-0.390 ± 0.009
25.5	-0.379 ± 0.009
26.0	-0.376 ± 0.009
26.5	-0.351 ± 0.009
27.0	-0.321 ± 0.008
27.5	-0.308 ± 0.008
28.0	-0.280 ± 0.008
28.5	-0.274 ± 0.008
29.0	-0.263 ± 0.008
29.5	-0.264 ± 0.008
30.2	-0.285 ± 0.008
Normalization uncertainty	± 1.6 %

FIGURE CAPTIONS

Fig. 1. Angular distributions of the proton polarization $p(\theta)$ and the differential cross-section $\sigma(\theta)$ at 20 and 22 MeV. Unless explicitly shown, the error bars are smaller than the size of the points.

Fig. 2. Angular distributions of the proton polarization $p(\theta)$ and the differential cross-section $\sigma(\theta)$ at 37 and 40 MeV. Unless explicitly shown, the error bars are smaller than the size of the points.

Fig. 3. Polarization excitation functions across the 23.4 MeV resonance corresponding to the $3/2^+$ level at 16.7 MeV in ^{5}Li. Only three of the fifteen angles investigated are presented. Unless explicitly shown, the error bars are smaller than the size of the points. The dashed lines serve only as a guide to the eye.

Fig. 4. Polarization excitation function at $\theta_{cm} = 102.2°$ across the broad anomaly near 30 MeV. Full circles and rectangles are our data, open circles are from Ref. 14, the full triangle is from Ref. 19, and the open triangle from Ref. 21. In the insert a cross-section excitation function for d-^{3}He elastic scattering[2] at $\theta_{cm} = 90°$ is plotted for comparison.

Fig. 5. Polarization contour map for p-^{4}He elastic scattering between 16 and 45 MeV. The part of the figure below 20 MeV has been drawn after Refs. 14 and 15.

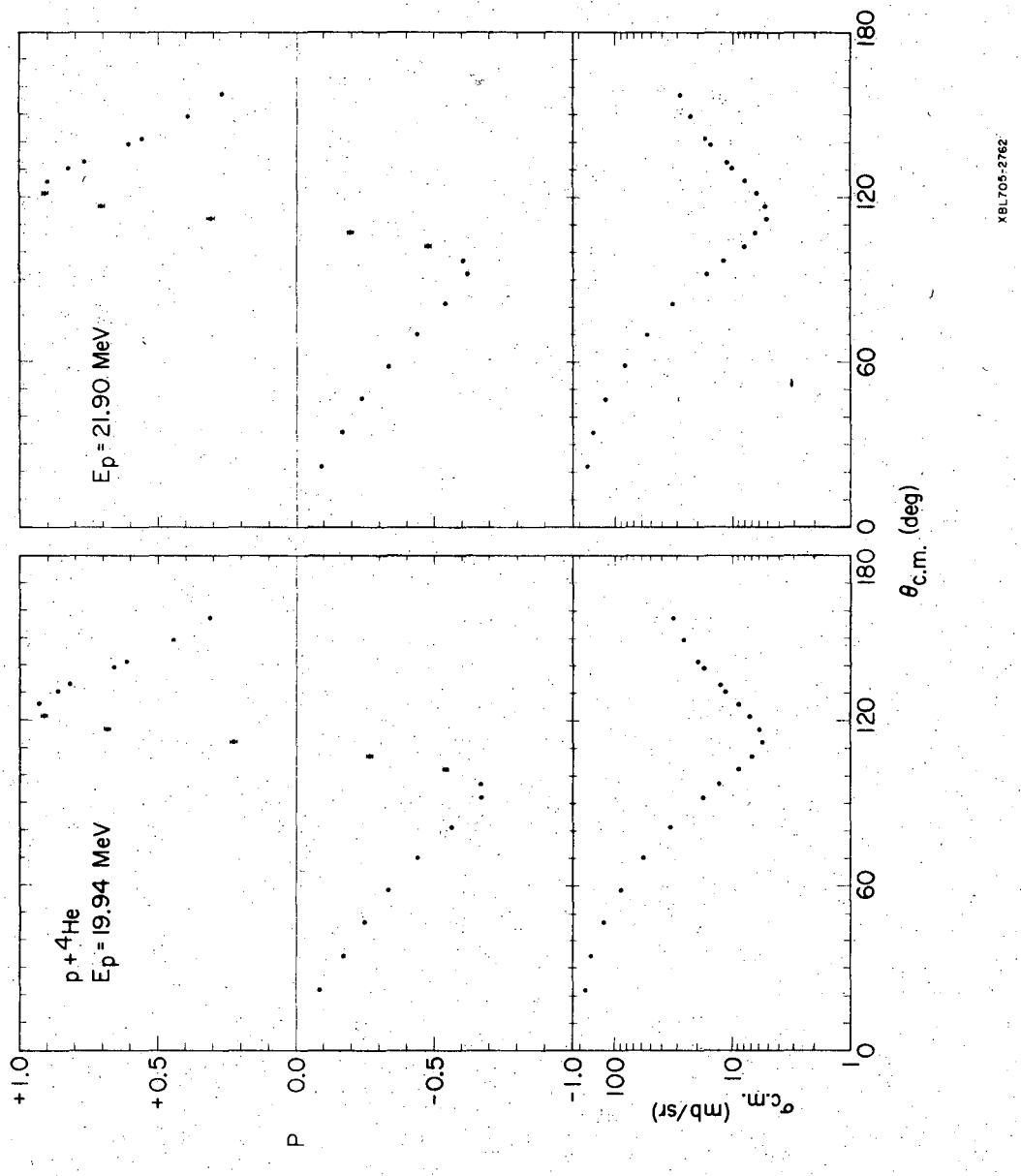
E_p = 21.90 MeV
p+^{4}He
E_p = 19.94 MeV
+1.0
+0.5
0.0
-0.5
-1.0
P
100
10
1
$\sigma_{c.m.}$ (mb/sr)
0
60
120
180
$\theta_{c.m.}$ (deg)
XBL705-2762

Fig. 1

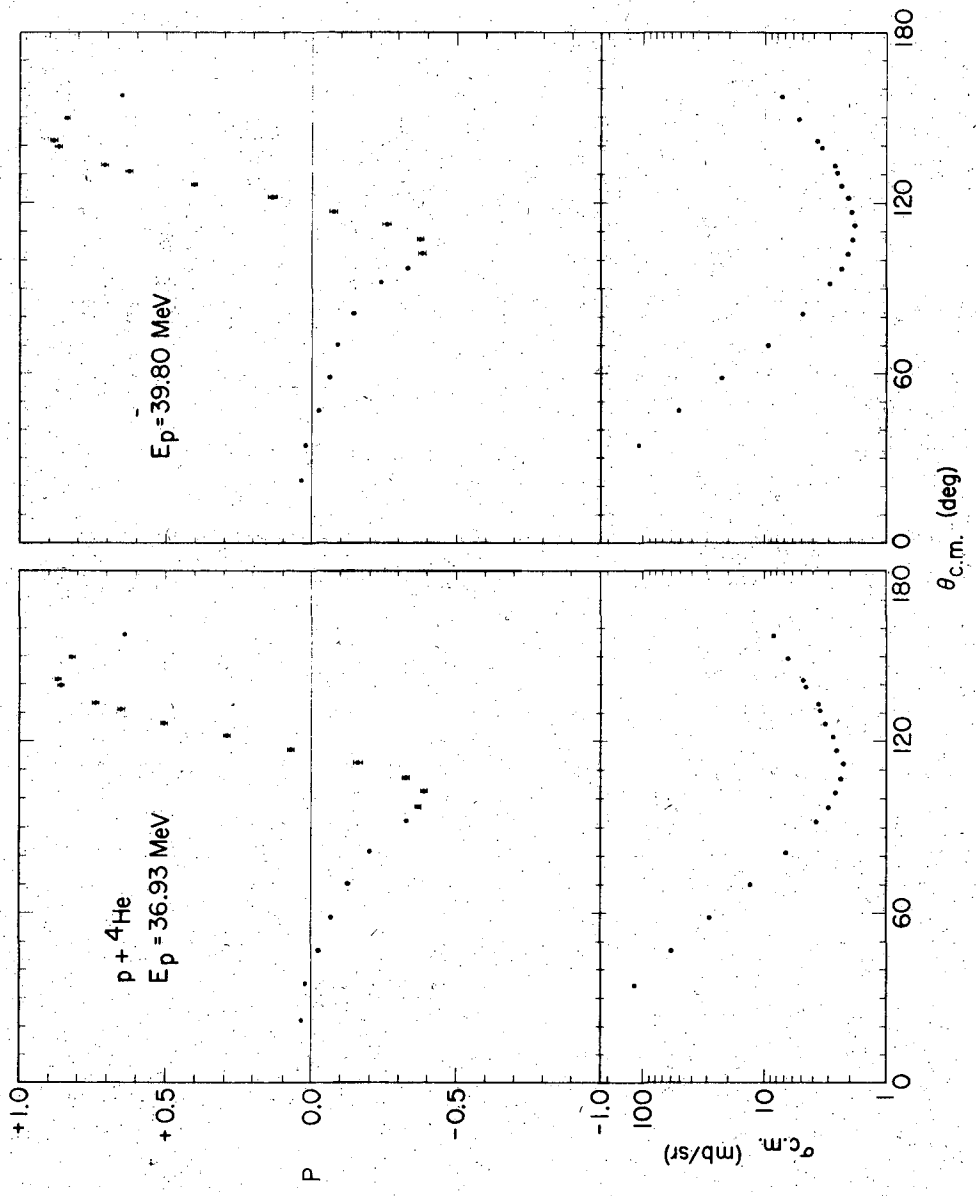
p + 4He
Ep = 36.93 MeV
Ep = 39.80 MeV
P
+1.0
+0.5
0.0
-0.5
-1.0
σc.m. (mb/sr)
100
10
1
θc.m. (deg)
0
60
120
180
XBL705-2764

Fig. 2

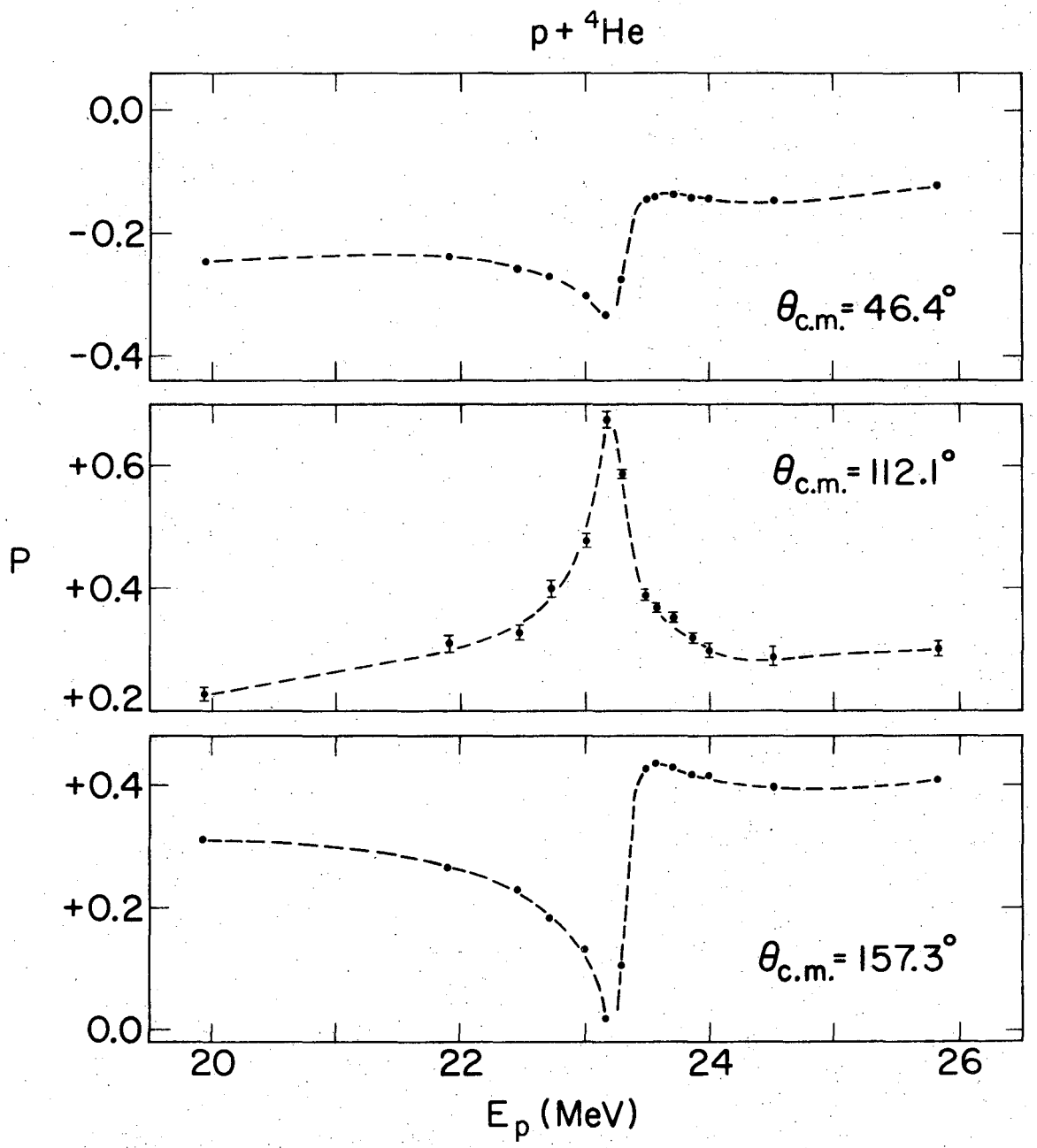

XBL704-2678

Fig. 3

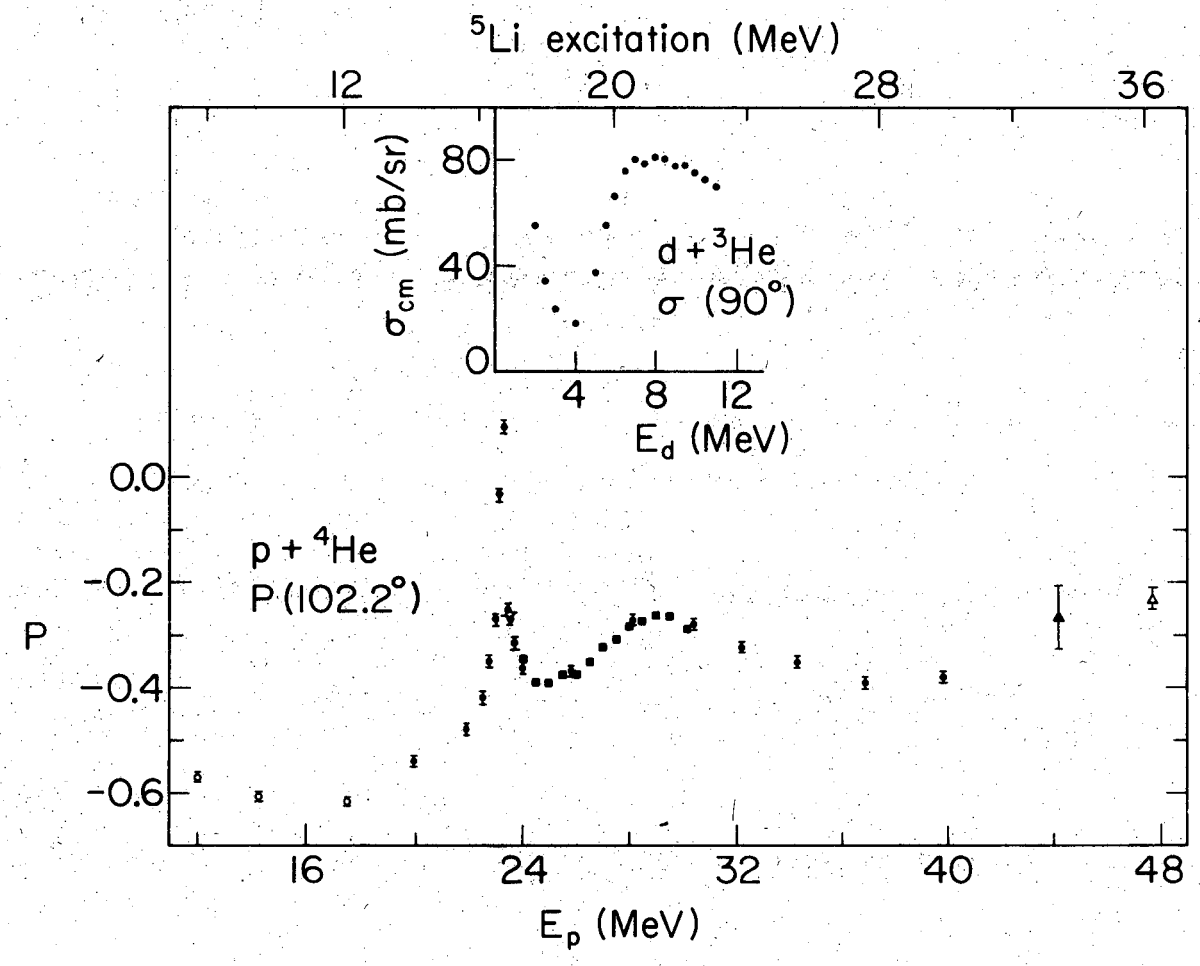

XBL703-2605

Fig. 4

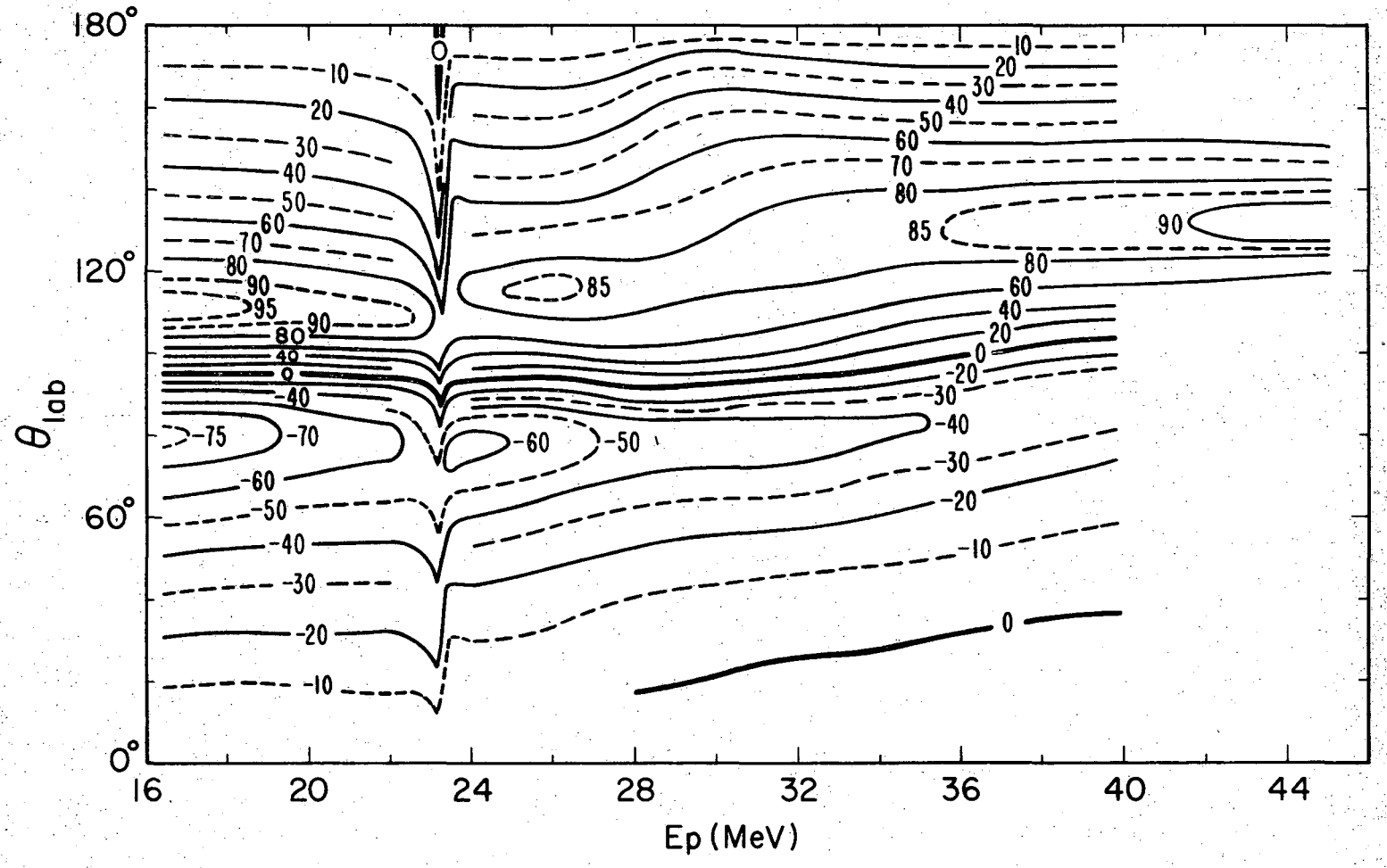

Fig. 5

TECHNICAL INFORMATION DIVISION
LAWRENCE BERKELEY LABORATORY
UNIVERSITY OF CALIFORNIA
BERKELEY, CALIFORNIA 94720